small methods

www.small-methods.com

Light Sources and Photodetectors Enabled by 2D Semiconductors

Jingzhi Shang, Chunxiao Cong, Lishu Wu, Wei Huang,* and Ting Yu**

The emerging 2D semiconductors have aroused increasing attention due to their fascinating fundamental properties and application prospects. Technical investigation of 2D semiconductor–based electronics and optoelectronics is paving the way to realizing practical applications, which opens up new opportunities to reshape the current semiconductor industry. Particularly, 2D semiconductor–based optoelectronics can be extensively utilized in the promising semiconductor and information industries, such as solid-state lighting, on-chip optical interconnects, quantum computing, and communication. Here, the research progress regarding the fabrication and characterization of rapidly growing light-emitting devices and photodetectors enabled by 2D semiconductors is reviewed. According to different emission mechanisms, 2D semiconductor–activated light sources are classified into four types: excitonic light-emitting diodes (LEDs), quantum LEDs, valley LEDs, and lasers. Moreover, photodetecting devices based on atomically thin MoS_2, other 2D semiconductors, and van der Waals heterostructures are discussed, where diverse device structures, performance parameters, and working principles are compared. Furthermore, the remaining challenges in the realization of practical devices with desirable features are outlined and new research opportunities for 2D semiconductor optoelectronics are proposed.

1. Introduction

The successful preparation of 2D metallic, semiconducting, and insulating crystals enables many opportunities for fundamental studies and device applications.[1–3] Since the experimental exploration of direct-bandgap monolayer (1L) MoS_2,[4,5] 2D semiconductors have rapidly drawn great attention from the global research communities of materials, physics, engineering, and chemistry.[6–8] Optical bandgaps of emerging 2D semiconductors such as 1L transition-metal dichalcogenides (TMDs),[9–14] 1L black phosphorous (BP),[15] ultrathin group III and IV chalcogenides (e.g., GaS and GeS),[16,17] and 1L hexagonal boron nitride (hBN),[18] cover the broad spectral range from ultraviolet to infrared wavelengths (**Figure 1**), which promotes the new development of photonic and optoelectronic applications.[17,19] These 2D semiconductors have exhibited many interesting properties like robust excitonic effects,[20] significant quantum confinement,[21] strong spin–orbit coupling,[22] and many-body interactions.[23] In particular, 1Ls of 2H-type MoS_2, $MoSe_2$, WS_2, and WSe_2 are direct-bandgap semiconductors, which are intrinsically suitable for light-emitting and photodetecting applications.[4,24–26] Meanwhile, atomically thin TMDs and their heterostructures have shown intriguing optical responses such as unique valley polarization,[27–29] room-temperature excitonic emission,[4] a wealth of excitonic states (e.g., trion, biexciton, dark exciton),[10,11,13,30,31] valley Zeeman splitting,[32–34] single-photon emission,[35–38] valley-selective optical Stark effect,[39] formation of exciton–polaritons,[40–42] and exciton–plasmon coupling.[43] Understanding of these effects is fundamentally important for developing high-performance optoelectronic devices with desirable and/or new features. Structurally, 2D semiconductors can be ultrathin, flexible, and transparent, which make them suitable for fabricating wearable optoelectronic devices. Moreover, controllable growth[44] and transfer techniques[45–47] of large-area 2D semiconductors make scalable and low-cost device fabrication practical. Technically, semiconductor-based light sources and photodetectors are two key elements for the realization of many prevailing optoelectronic applications, such as general illumination devices, various light indicators, optical storage, light sensing, optical interconnects, optical isolators, and optical

Dr. J. Shang, Prof. W. Huang
Shaanxi Institute of Flexible Electronics (SIFE)
Northwestern Polytechnical University (NPU)
127 West Youyi Road, Xi'an 710072, P. R. China
E-mail: iamwhuang@nwpu.edu.cn

Dr. J. Shang, L. Wu, Prof. T. Yu
Division of Physics and Applied Physics
School of Physical and Mathematical Sciences
Nanyang Technological University
21 Nanyang Link, Singapore 637371, Singapore
E-mail: yuting@ntu.edu.sg

Prof. C. Cong
State Key Laboratory of ASIC and System
School of Information Science and Technology
Fudan University
220 Handan Rd., Yangpu District, Shanghai 200433, P. R. China
E-mail: cxcong@fudan.edu.cn

Prof. W. Huang
Key Laboratory of Flexible Electronics (KLOFE) & Institute of Advanced Materials (IAM)
Nanjing Tech University (NanjingTech)
30 South Puzhu Road, Nanjing 211800, P. R. China

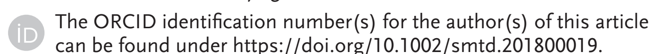
The ORCID identification number(s) for the author(s) of this article can be found under https://doi.org/10.1002/smtd.201800019.

DOI: 10.1002/smtd.201800019

© 2018 WILEY-VCH Verlag GmbH & Co. KGaA, Weinheim

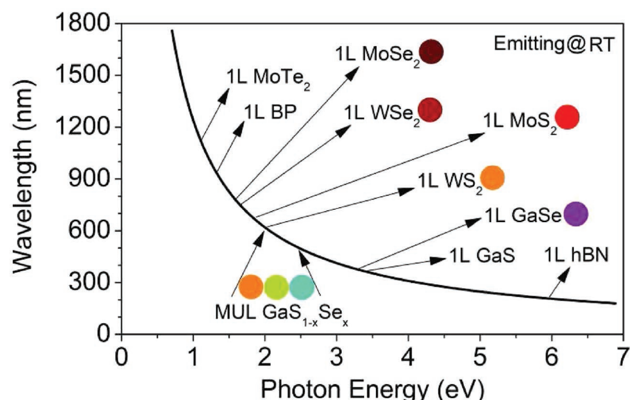

Figure 1. Optical bandgaps of representative 2D semiconductors at room temperature (RT) and the corresponding emission covering ultraviolet to near-infrared wavelengths. MUL represents multilayer. Optical bandgaps are estimated according to previous studies.[9–16,18]

and quantum communication, which have large industrial markets and great economic potential. With the development of material preparation and investigation of optoelectronic properties of 2D semiconductors, many efforts have been made toward light-emitting and photodetecting applications. Consequently, various light-emitting diodes (LEDs),[24,48–50] lasers,[51,52] and photodetectors[25,53] have been demonstrated by use of 2D semiconductors and their van der Waals (vdW) heterostructures as active media.

Here, we focus on the research progress on two classes of 2D-semiconductor-enabled optoelectronic applications: light sources and photodetectors. More specifically, four types of lighting devices are discussed according to their emission characteristics. Moreover, 2D semiconductor–based photodetectors are reviewed and compared in terms of different active materials. Subsequently, we list the remaining challenges in the development of these optoelectronic devices and highlight the exciting research opportunities.

2. 2D Semiconductor–Activated Light Sources

Semiconductor light-emitting devices are the fundamental building blocks of many modern optoelectronic applications, such as optical communication, quantum information, optical data storage, lighting, displays, and indicators. In general, in contrast to conventional light sources like incandescent lambs, fluorescent tubes, and gas and solid-state lasers, semiconductor light sources have competitive advantages, including low power consumption, long lifetime, stable output, and so on. The rising 2D semiconductors are providing a new material platform to boost the development of next-generation light-emitting devices with the attractive features of ultrathin thickness, compactibility, flexibility, transparency, and excellent compatibility with integrated-circuit manufacturing technology. Here, we outline four types of the most promising light sources: excitonic 2D-semiconductor-based LEDs (2DLEDs), quantum 2DLEDs, valley 2DLEDs, and 2D semiconductor lasers.

Chunxiao Cong received her B.Sc. degree from the Northeast Normal University (China) in 2004. She received her M.Sc. degree and Ph.D. degree from the Jilin University (China) in 2007 and the Nanyang Technological University (Singapore) in 2012, respectively. After a research fellowship at the Nanyang Technological University (Singapore), she joined the Fudan University as the National Thousand Youth Talents Plan Professor of China in 2015. Her main research interests are optical and material properties of 2D layered materials and their applications in nanoelectronics, optoelectronics, and flexible electronics.

Wei Huang is Academician of the Chinese Academy of Sciences, Foreign Academician of the Russian Academy of Sciences, Fellow of the Royal Society of Chemistry and Fellow of the Optical Society of America. He received his B.Sc., M.Sc., and Ph.D. from the Peking University. He then carried out his postdoctoral research at the National University of Singapore and participated in the foundation of the Institute of Materials Research and Engineering. He is now Deputy President and Provost of the Northwestern Polytechnical University, China. His current research interests include organic/plastic/flexible electronics, bioelectronics, nanomaterials, nanoelectronics, and polymer chemistry.

Ting Yu is a professor in the School of Physical and Mathematical Sciences at the Nanyang Technological University (Singapore). He received his B.Sc. degree from the Jilin University (China) in 1999 and his Ph.D. degree from the National University of Singapore in 2003. His current research focuses on low-dimensional, especially 2D, materials, and investigation of their optical, optoelectrical, and electrochemical properties for developing novel electronics, optoelectronics, and energy conversion/storage devices.

© 2018 WILEY-VCH Verlag GmbH & Co. KGaA, Weinheim

2.1. Excitonic 2DLEDs

With the dimensional reduction of semiconductor crystals, a strong excitonic effect and quantum confinement can be expected,[20,23,54] which may enable efficient excitonic emission at room temperature (RT). Indeed, large exciton binding energies have been observed for ultrathin layered TMDs such as 1L MoS_2, WS_2, $MoSe_2$, and WSe_2.[55] Meanwhile, stable exciton emission with high quantum efficiency in 2D semiconductors prepared by both mechanical exfoliation and chemical vapor deposition (CVD) techniques has been obtained via superacid treatment at RT.[56–58] Thus, developing highly efficient light-emitting devices based on 2D semiconductors is practical and promising. In 2013, Sundaram et al. reported excitonic electroluminescence (EL) generated around the contact region between 1L MoS_2 and a Cr/Au electrode in a field-effect transistor (**Figure 2**a), in agreement with photoluminescence (PL) and absorption data (Figure 2b), where the hot-carrier processes were considered to be the main emission mechanism.[24] By creating vertical p–n junctions consisting of n-type 1L MoS_2 and p-type bulk silicon (Figure 2c), EL due to excitons, trions, bound excitons, and excited excitons has been observed at RT (Figure 2d) and low temperatures,[59,60] where Auger recombination via exciton–exciton annihilation has contributed to the bound exciton emission.[60] With the closely arranged dual-gate configurations, excitonic EL has been obtained from in-plane p–n junctions of 1L WSe_2 flakes formed under the proper electrostatic doping,[48,61,62] representing a major step

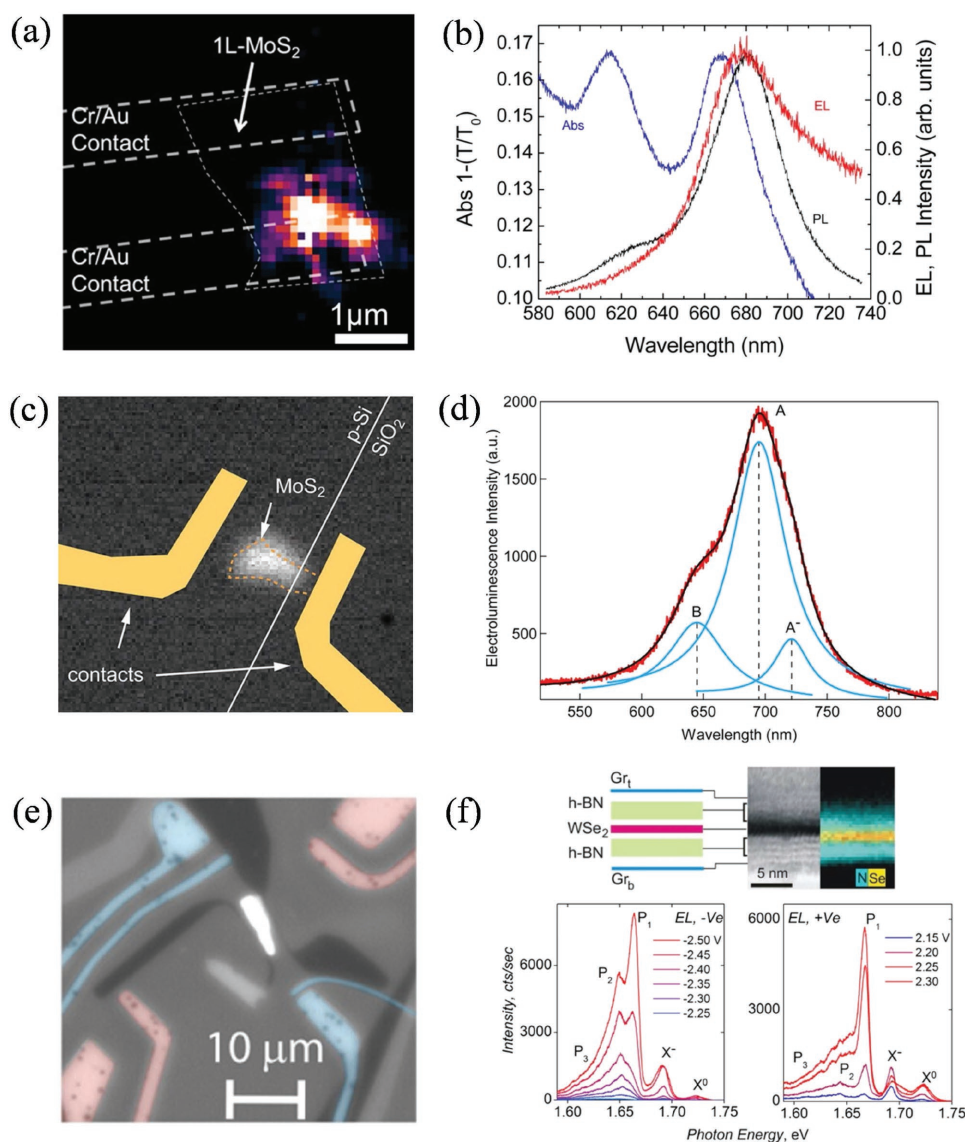

Figure 2. a,b) EL intensity image of a 1L MoS_2 field-effect transistor (a), and the corresponding absorption, PL, and EL spectra (b). a,b) Reproduced with permission.[24] Copyright 2013, American Chemical Society. c,d) EL intensity image of an n-MoS_2/p-Si heterojunction (c) and its EL spectrum with three fitting components (d). c,d) Reproduced with permission.[59] Copyright 2014, American Chemical Society. e,f) False color image of a WSe_2 LED (e), and its device structure with EL spectra collected at negative and positive voltages (f). e,f) Reproduced with permission.[63] Copyright 2015, American Chemical Society.

© 2018 WILEY-VCH Verlag GmbH & Co. KGaA, Weinheim

Table 1. Excitonic LED–based 2D semiconductors.

Device structure	Observed EL λ; temperature [nm]; [K]	Threshold; EL efficiency	Dominant emission mechanism	Reference
1L MoS_2[a)]/metal (Cr/Au)	580–740; NA	15 kW cm^{-2}; NA	Hot-carrier effect	[24]
n-type 1L MoS_2[a)]/p-Si	550–800; RT	3.2 W cm^{-2}; NA	p–n junction	[59]
n-type 1L MoS_2[a)]/p-Si	500–800; RT, 10 K	15 µA; NA	p–n junction	[60]
1L WSe_2[a)] with dual gates	710–800; RT, 60 K	<0.2 nA; NA	p–n junction	[48]
1L WSe_2[a)] with dual gates	700–800; RT	NA; 1%	p–n junction	[61]
1L WSe_2[a)] with dual gates	690–1000; RT	NA; 0.1%	p–n junction	[62]
Graphene/multiple quantum wells of MoS_2[a)]–hBN/graphene	620–880; RT–6 K	1.8 nA µm^{-2}; 8.4%	Quantum-well emission	[49]
Graphene/hBN/1L WSe_2[a)]/hBN/graphene	690–825; RT–6K	NA; 5%	Quantum-well emission	[63]
1L and 2L WS_2[a)] with ion liquid gate	560–890; NA	NA	p-n junction	[64]
Multilayer MoS_2[a)]/Al_2O_3/GaN	485–850; RT	NA; 0.01%	Electric-field effect	[68]
Graphene/hBN/1L WSe_2[a)]/hBN/graphene/nanocavity	710–790; RT	NA; 0.2%	Carrier tunneling	[69]

[a)]Exfoliated samples.

toward the development of electrically tunable 2DLEDs. By alternatively stacking 1L MoS_2 or WS_2 and hBN layers, single- and multiple-quantum-well structures have been prepared to realize relatively high efficiency EL (i.e., ≈8.4%) at 6 K, where graphene layers have been employed as contacting electrodes.[49] Enhanced EL brightness via carrier tunneling was observed from single-quantum-well LEDs employing 1L WSe_2 as the emitting medium (Figure 2e,f); the external quantum efficiency increased with the temperature and reached 5% at RT, which is unlike the typical behavior of 1L $MoSe_2$ and MoS_2 LEDs with similar structures, owing to the reverse band alignments of the bottom conduction-band states.[63] By employing the ion-liquid-gated field-effect configuration, EL from 1L and 2L WS_2 was realized, where electrons and holes were accumulated at a proper gate voltage around two opposite contact regions, respectively.[64] Moreover, EL from the suspended MoS_2 transistor was demonstrated under ambipolar injection, where the emission mechanism was attributed to the Joule heating effect.[65] Field-emission tunnel diodes based on 1L WS_2 were demonstrated by use of the metal–insulator (BN)–semiconductor configuration, where excitonic EL with a quantum efficiency of ≈1% was observed at a very low current density of several pA µm^{-2}.[66] The vertical heterojunction of p-type 1L or 2L WSe_2 and n-type few-layer MoS_2 was used to realize EL, where hot-electron luminescence and indirect-bandgap emission were also identified in addition to the exciton emission.[67] Furthermore, with the vertically stacked heterostructures made of multilayer MoS_2 or WSe_2, Al_2O_3, and GaN, unconventionally electric-induced EL associated with the direct excitonic transition has been observed from multilayer MoS_2 or WSe_2,[68] which paves the way to the development of atomically thin LEDs based on multilayer indirect-bandgap semiconductors. By integrating a 1L WSe_2 LED with a photonic-crystal cavity, enhanced EL was realized and high-speed modulation was achieved.[69] In addition, with the help of an electrolyte film, centimeter-scale LEDs based on 1L WSe_2 and MoS_2 have been accomplished, which takes an important step toward the realization of large-area lighting applications based on 2D semiconductors.[70] As illustrated above, excitonic EL in atomically thin semiconductors with direct or indirect bandgaps has been demonstrated at different experimental conditions by use of diverse device structures and **Table 1** illustrates the details of device structure, emitting wavelength, operation temperature, threshold, efficiency, and emission mechanism for comparison.

2.2. Quantum 2DLEDs

Single-photon emission from solid-state material systems is very promising for the development of next-generation quantum-information technologies[71] such as quantum computing,[72] quantum teleportation,[73] and quantum cryptography.[74] Since 2015, optically pumped quantum emission from atomically thin materials[35–38,75] has aroused rising attention from the global research communities of 2D materials and quantum optics. Moreover, some efforts have been made to achieve electrically driven quantum LEDs based on 2D semiconductors. With a vertically stacked architecture consisting of graphene, few-layer hBN, and TMD layers (e.g., 1L WSe_2), narrow quantum emission was demonstrated under electrical pumping at 10 K, where electrons were injected from the graphene to the TMD layers by passing the tunnel barrier of the ultrathin hBN (**Figure 3**a–d).[76] The defective nature and the doublet features of the quantum emission from vertical graphene/hBN/TMD layers/hBN/graphene junctions have been revealed at low operation voltages (e.g., 2 V) and low temperature (Figure 3e–g).[77,78] Meanwhile, quantum light from the lateral LED based on 1L WSe_2 was realized, where split back gates were employed to form the in-plane p–i–n junctions.[78] In practice, such quantum 2DLEDs can be very promising for many on-chip quantum information applications.

2.3. Valley 2DLEDs

Strong spin–orbit coupling of 1L TMDs results in the large band splitting in the valance and conduction bands, enabling unique valleytronic properties. By using the electric-double-layer transistor configuration together with a gated ionic liquid,

© 2018 WILEY-VCH Verlag GmbH & Co. KGaA, Weinheim

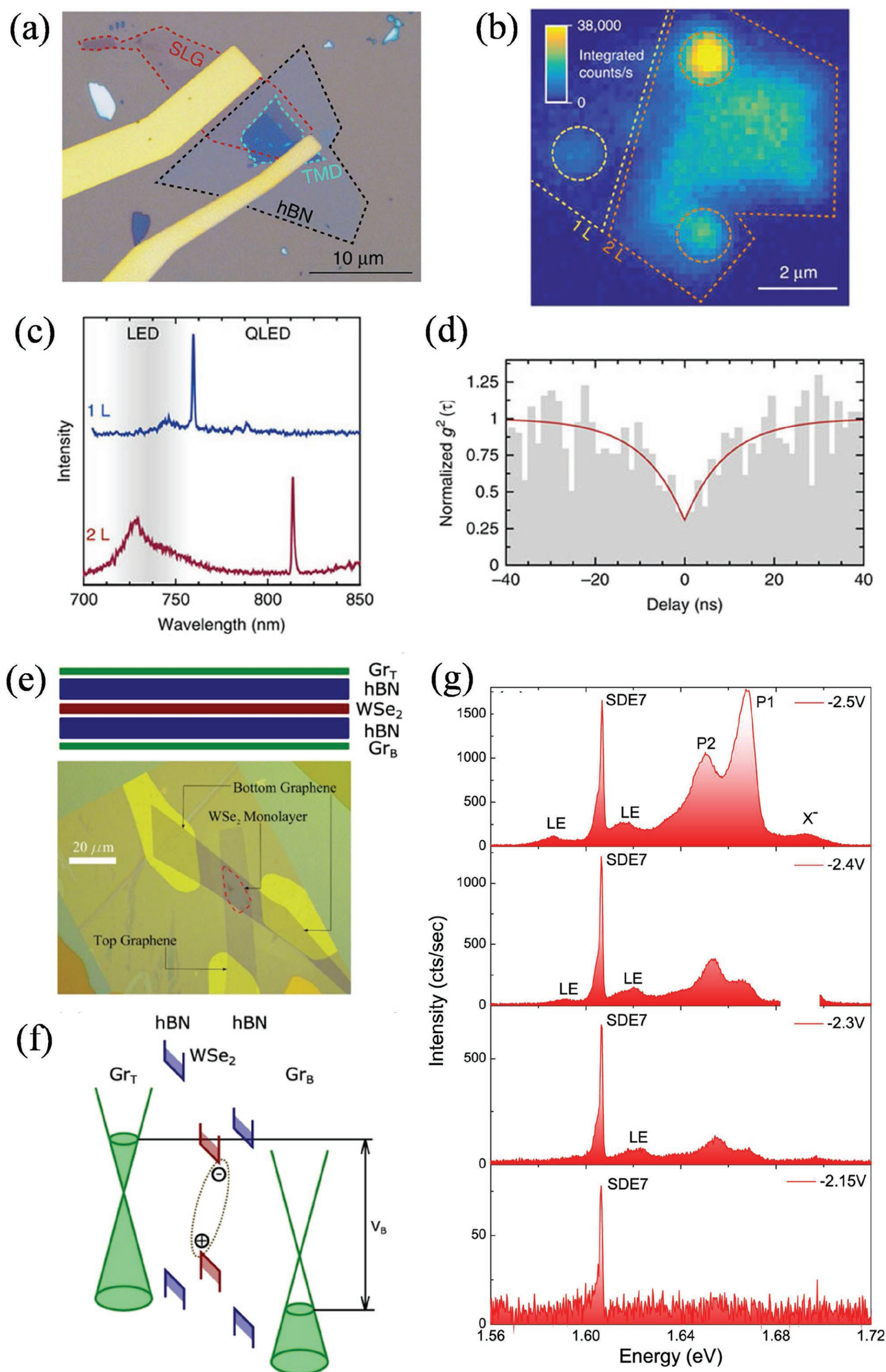

Figure 3. a,b) Optical image of a WSe_2-based QLED (a), and EL intensity image (b). c) EL spectra from 1L and 2L WSe_2 quantum emitters. d) Second-order correlation measurement of a WSe_2 quantum emitter. a–d) Reproduced with permission.[76] Copyright 2016, Springer Nature. e) Schematic of the device structure and optical image. f) Band alignment of the heterostructure of graphene/hBN/1L WSe_2/hBN/graphene under a bias voltage. g) EL spectra from single-defect light emitters at various voltages. e–g) Reproduced with permission.[77] Copyright 2016, IOP Publishing.

valley-polarized EL from 1L and few-layer WSe_2 was demonstrated and explained in terms of different electron–hole overlaps caused by the electric fields, which was switchable under the opposite current-injection directions.[50] Moreover, with a similar device structure except for the emitting material, EL from 1L $MoSe_2$ with a high circular polarization (i.e., 66%) was

© 2018 WILEY-VCH Verlag GmbH & Co. KGaA, Weinheim

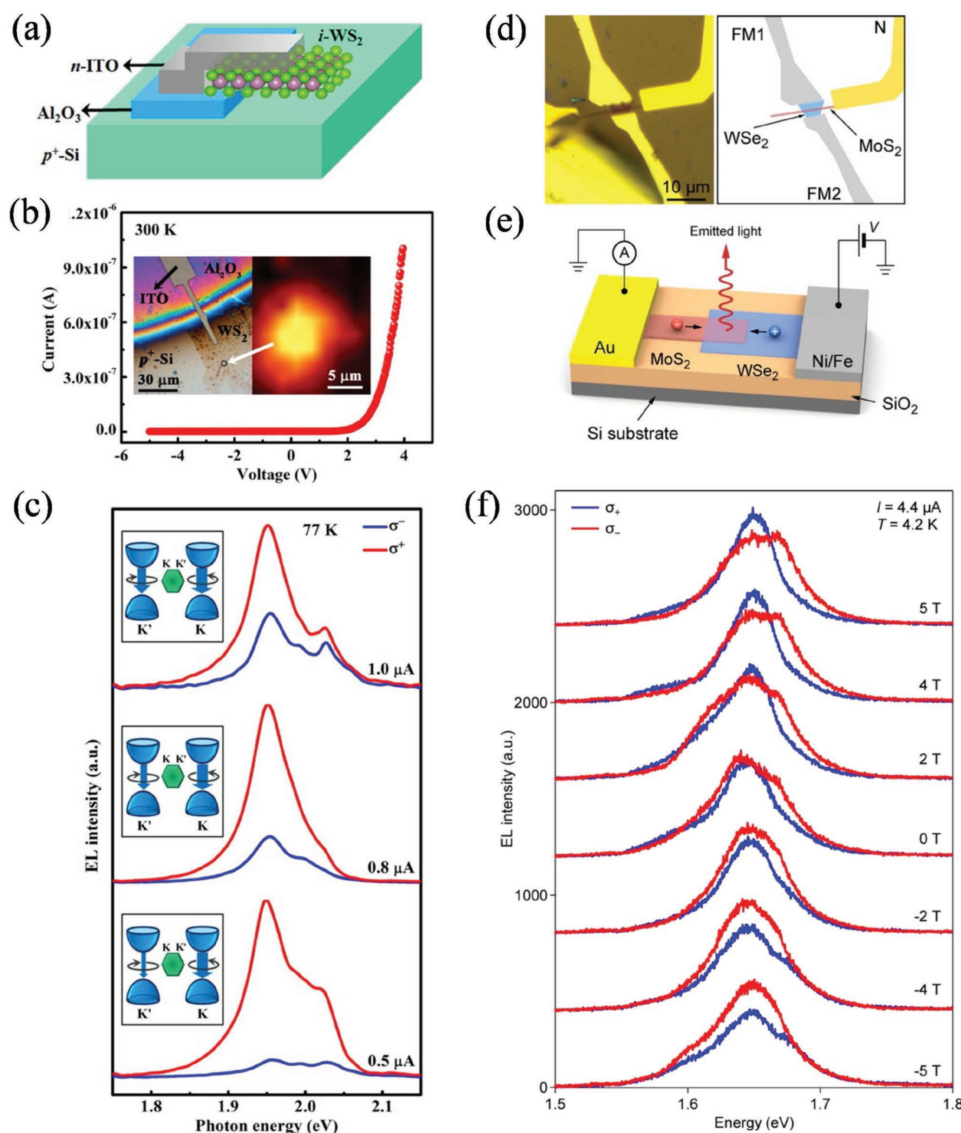

Figure 4. a) Schematic of a valley LED based on the p-Si/i-1L WS_2/n-ITO junction. b) *I–V* curve with optical and EL images. c) Valley-polarized EL collected at three injection currents. a–c) Reproduced with permission.[80] Copyright 2016, American Chemical Society. d) Optical image and the corresponding diagram of a heterojunction of 1L MoS_2/1L WSe_2. e,f) Schematic and circularly polarized EL under different magnetic fields of an LED based on a heterojunction of 1L MoS_2/1L WSe_2, respectively. d–f) Reproduced with permission.[28] Copyright 2016, American Chemical Society.

achieved, where the mechanism of the valley polarization of the EL was found to be different from that of the low valley polarization of PL associated with ultrafast intervalley scattering.[79] By employing scalable CVD-grown 2D semiconductors, an electrically tunable LED consisting of p-Si, 1L WS_2, and n-type indium tin oxide (ITO) layers has been realized (**Figure 4**a–c), which indicates the practicality of large-scale production of circularly polarized optoelectronic devices.[80] Circularly polarized EL was observed in a vertical p-(Ga, Mn)As/n-WS_2 diode, where the dilute ferromagnetic semiconductor of (Ga, Mn) As acted as a spin-injection layer under out-of-plane magnetic fields.[81] Furthermore, by injecting spin-polarized charge carriers from the ferromagnetic electrode, valley-polarized EL from an LED made of the heterostructures of 1L WSe_2 and MoS_2 was obtained under external magnetic fields (Figure 4d–f), where the spin–valley locking in the 1L WSe_2 played a key role in the observed valley polarization.[28]

2.4. 2D Semiconductor Lasers

Semiconductor lasers are playing key roles in many practical applications, such as optical communication, on-chip optical interconnects, laser printing, and data storage and reading. Owing to their unique structural and optical properties, making 2D semiconductor lasers is very attractive, where new features (e.g., ultrathin and flexible) and functionalities (e.g., valley-selective lasing) can be expected. Recently, optically pumped point[51] and edge-emitting[52,82] dominant lasers based on 1L and few-layer TMDs have been demonstrated. In

 © 2018 WILEY-VCH Verlag GmbH & Co. KGaA, Weinheim

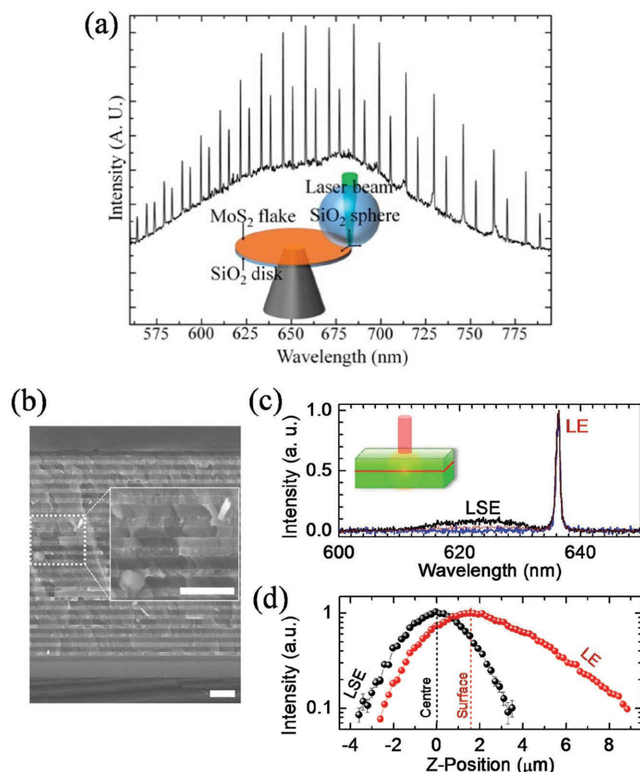

Figure 5. a) Multimode lasing of 4L MoS_2–based lasers employing a microsphere–microdisk resonant cavity. Reproduced with permission.[82] Copyright 2015, American Chemical Society. b) Cross-sectional scanning electron microscopy (SEM) image of a 1L WS_2–activated VCSEL. c) Normalized PL spectra taken at the cavity center (black), the top surface (red), and 5.1 µm above the cavity center (blue). d) Normalized integrated PL intensity of LE and LSE at different Z-positions; LE and LSE in (c) and (d) represent lasing emission and leakage spontaneous emission, respectively. b–d) Reproduced with permission.[84] Copyright 2017, Springer Nature.

detail, ultralow threshold and continuous-wave (CW) lasing of 1L WSe_2 was obtained at temperatures below 160 K by using a photonic-crystal nanocavity.[51] At 10 K, 1L WS_2 lasing was achieved with a microdisk resonator and under the excitation of a femtosecond pulsed laser.[52] By employing a coupled microdisk–microsphere cavity, multiple CW lasing peaks have been observed from few-layer MoS_2 at RT (**Figure 5**a).[82] Previously, in view of the intense and nonblinking PL of 1L WS_2 together with its planar nature, 2D semiconductors were proposed to be employed as the active medium to realize vertical-cavity surface-emitting lasers (VCSELs).[83] Consequently, room-temperature single-mode 2D lasing from a 1L WS_2 in an ultimately thin ($\lambda/2$) vertical cavity has been achieved under CW ultralow-power photoexcitation (Figure 5b–d), where the fabrication techniques are compatible with conventional planar technology.[84] By use of the Si-based photonic-crystal nanobeam cavity, excitonic lasing from 1L $MoTe_2$ has been realized in the infrared spectral range (≈1132 nm) at RT, which opens up a new material platform to develop on-chip nanolaser sources for Si-based nanophotonic applications.[85] Moreover, RT low-threshold lasing of few-layer $MoTe_2$ on the Si photonic crystal nanocavity has been demonstrated at an emission wavelength of 1305 nm, which is suitable for conventional fiber-optic communication.[86] For a better comparison, **Table 2** shows the information of active medium, resonant cavity structure, operation temperature, working mode, and threshold of the 2D semiconductor lasers described above.

Table 2. 2D semiconductor lasers.

Sample	Resonant cavity structure	Operation temperature; mode	Threshold	Reference
1L WSe_2	Photonic-crystal nanocavity	80–160 K; CW	1 W cm^{-2}	[51]
1L WS_2	Microdisk cavity	10 K; pulsed	5–8 MW cm^{-2}	[52]
4L MoS_2	Microsphere–microdisk	RT; CW	7.1 kW cm^{-2}	[82]
1L $MoTe_2$	Silicon nanobeam cavity	RT; CW	6.6 W cm^{-2}	[85]
1L WS_2	Vertical cavity	RT; CW	0.44 W cm^{-2}	[84]
4 nm $MoTe_2$	Photonic crystal nanocavity	RT; CW	1.5 kW cm^{-2}	[86]

3. 2D Semiconductor–Based Photodetectors

Photodetecting devices are key elements for semiconductor-based optoelectronic applications such as on-chip optical interconnects and optical communications. 2D semiconductors and their vdW heterostructures absorb light ranging from the ultraviolet to infrared regions, which provides a new playground for the development of next-generation photodetectors. Diverse device structures have been employed to achieve a high-performance photoresponse, typically including 2–4 electrodes, dielectric layers, and 2D semiconductors or their heterostructures. The active regions of these photodetectors can be made by 2D semiconductors or vdW heterostructures, where p–n, p–i–n, or Schottky junctions often form to realize charge separation. Direct contacts with the active regions can be conventional metal electrodes or ultrathin graphene layers, where the Fermi level of graphene electrodes can be electrically or chemically controlled to reduce the contact resistances; thus, the collection efficiency of photocarriers can be enhanced.[53,87–89] Typical generation mechanisms of a photoresponse from 2D materials include photovoltaic, photogating, photo-thermoelectric, and photobolometric effects.[90–92] In general, the key performance metrics to evaluate photodetectors include the photoresponsivity, the spectral region for the photodetection, the response time, and the external quantum efficiency.[93–95] Moreover, other important parameters have also been introduced to characterize the device performance, such as on–off current ratio, detectivity, photogain, and noise equivalent power.[94,96–99]

3.1. MoS_2 Photodetectors

Since 2010, atomically thin MoS_2, as one of the most representative 2D semiconductors, has aroused increasing attention for its fundamental physics and optoelectronic applications.[4,26,100,101] 1L and multilayer MoS_2 are direct- and indirect-bandgap semiconductors, respectively, which promote the development of high-performance photodetection devices

 © 2018 WILEY-VCH Verlag GmbH & Co. KGaA, Weinheim

operating in the visible and infrared spectral ranges. 1L MoS_2 with two separate electrodes can be used to form a simple phototransistor, where the photoresponse is monitored by measuring the photocurrent or the photovoltage. Such 1L MoS_2 phototransistors with fast photoswitching and good stability were demonstrated by Yin et al. (**Figure 6**a–d),[25] presenting better photoresponsibility than graphene-based photodetectors with similar device configurations.[102] Moreover, an ultrasensitive photoresponse of 1L MoS_2 phototransistors was realized in the broad spectral range from 400 to 680 nm, where a maximum photoresponsivity of 880 A W^{-1} was found at 561 nm.[103] In general, the spectral photoresponsivity of a semiconductor strongly depends on its optical bandgap. As is known, the optical bandgaps of MoS_2 layers are thickness-dependent, and thus varied photodetecting capabilities can be expected in MoS_2 layers with different thicknesses. Indeed, 1L and 2L MoS_2 phototransistors present good photoresponsivities to green light, while 3L MoS_2 phototransistors show better photoresponse to red light.[104] Furthermore, multilayer MoS_2 phototransistors with high photoresponsivity (>100 mA W^{-1}) have also been fabricated, showing a broad photoresponse from the visible to near-infrared wavelengths.[97] By employing a top-gate ferroelectric material and 3L MoS_2, a photodetector with good detectivity ($\approx 2.2 \times 10^{12}$) and ultrahigh photoresponsivity (2570 A W^{-1}) was demonstrated in the broad range from the visible region to 1550 nm.[105] Except the mechanically exfoliated MoS_2 samples used in previous studies,[25,97,102–104] CVD-grown 1L and few-layer MoS_2 have also been adopted to fabricate phototransistors.[96,106,107] In particular, to obtain high-performance CVD-grown 1L MoS_2 phototransistors, the air-adsorption effect needs to be taken into account, where air adsorbates at the surface and the MoS_2/substrate interface could result in the decrease of the photoresponsivity and the photocurrent decay time.[106] With interdigitated Au electrodes and few-layer CVD-grown MoS_2, high-performance broadband phototransistors were demonstrated in harsh environments (Figure 6e–h), where the photoresponsivity, detectivity, and photogain reached 0.57 A W^{-1}, $\approx 10^{10}$ cm $Hz^{1/2}$ W^{-1}, and 13.3, respectively.[96] Interestingly, a selective spin–valley-coupled photocurrent in a CVD-grown 1L MoS_2 phototransistor has been observed, where the circular photogalvanic effect at resonant excitations was found to be the dominant reason for the large photocurrent dichroism of 60%.[108] To compare more quantitatively, the details of working medium, photoresponsivity, response time, and wavelength for detection response of various MoS_2 photodetectors are shown in **Table 3**.

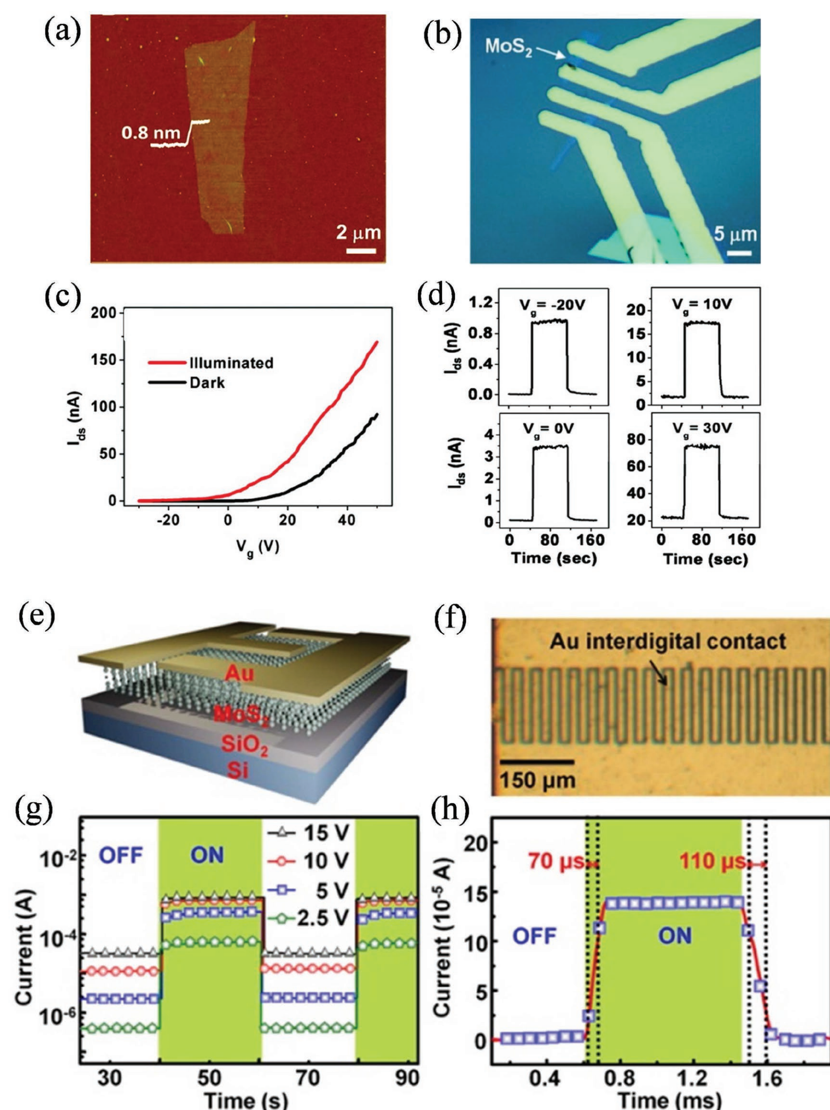

Figure 6. a,b) Optical images of an exfoliated 1L MoS_2 and the corresponding field-effect transistor. c) Drain–source current versus gate voltage collected under dark (black) and illuminated (red) conditions. d) Photoswitching behaviors observed at varied gate voltages. a–d) Reproduced with permission.[25] Copyright 2012, American Chemical Society. e,f) Schematic and optical image of field-transistors based on CVD-grown 3L MoS_2. g) Photocurrent as a function of time collected at different voltages. h) Fast photoresponse observed in a short time period and at 5 V. e–h) Reproduced with permission.[96] Copyright 2013, American Chemical Society.

3.2. Photodetectors Based on Other 2D Semiconductors

Beyond MoS_2 photodetectors, many efforts have been made to develop photodetecting devices based on other 2D semiconductors, including ultrathin layers of WS_2,[111,112] $MoSe_2$,[113] WSe_2,[61,62] BP,[114,115] GaTe,[99,116] GaSe,[117–119] GaS,[120] In_2Se_3,[98] $ReSe_2$,[121] and SnS_2.[122] Typical performance parameters of these devices are presented in **Table 4** for analysis. In 2014, low-temperature photoresponse behaviors of both exfoliated and CVD-grown 1L WS_2 were investigated (**Figure 7**a–d), where the photodetection abilities were significantly affected by the material

© 2018 WILEY-VCH Verlag GmbH & Co. KGaA, Weinheim

Table 3. Performance parameters of MoS_2 photodetectors.

Sample	Photoresponsivity [mA W^{-1}]	Response time [ms]	Detecting λ [nm]	Reference
1L MoS_2 a)	7.5	<50	Visible ≥ 400	[25]
1L MoS_2 a)	8.8×10^5 at 561 nm	600–9000	400–680	[103]
1L MoS_2 a)	5×10^4	<1	640	[109]
1L MoS_2 b)	>2.2×10^6 at 532 nm	55–5×10^5	532	[106]
1L MoS_2 b)	1.1 at 514.5 nm	<1000	488; 514.5	[107]
1L MoS_2 b)	3.07	<10	633	[110]
3L MoS_2 a)	2570 at 635 nm	1.8–2	Visible to 1550	[105]
35 nm MoS_2 a)	50–120 in visible	<2000	455–850	[97]
Multilayer MoS_2 b)	570 at 532 nm	0.07–0.11	400–700	[96]

a)Exfoliated samples; b)CVD-grown samples.

quality.[112] Several multilayer WS_2 phototransistors have shown high on/off ratios (≈10^5),[123] fast response times (5.3 ms),[111] good gas sensitivities,[124] and broadband photoresponse in the visible range.[111] By employing the electric-double-layer transistor configuration with controllable doping, a phototransistor based on CVD-grown 1L $MoSe_2$ with slight n-type doping presented a fast response time (<25 ms) at RT in ambient atmosphere (Figure 7e), which was significantly shorter than that (i.e., 30 s) of a phototransistor using heavily n-doped 1L MoS_2 grown by CVD (Figure 7f).[113] 1L WSe_2 phototransistors with dual back-gate electrodes were demonstrated, where the light–power conversion efficiencies reached 0.2–0.5% and the internal photoresponsivities were more than 200 mA W^{-1}.[61,62] Besides the TMD-based photodetectors mentioned above, the photoresponse properties of ultrathin BP have also drawn attention owing to the widely tunable bandgaps. As is known, the optical bandgap of BP layers depends on their thickness, corresponding to very broad spectral regions (i.e., 600 nm to 4 μm).[19] Visible and infrared photoresponse (e.g., 532–1550 nm) has been demonstrated by phototransistors using BP layers with different thicknesses, where the representative response time is about 1 ms.[114,115] Furthermore, photodetectors based on ultrathin semiconducting group-III chalcogenides have been studied.[98,116,120,125] In 2014, an ultrahigh photoresponsivity of ≈10^4 A W^{-1} was achieved in a multilayer GaTe phototransistor, which is one or two order higher than that for typical MoS_2 and Si phototransistors.[116] Phototransistors employing multilayer GaSe,[125] GaS,[120] and In_2Se_3[98] were prepared to realize an ultraviolet photoresponse (e.g., 254 and 300 nm), where an extraordinary external quantum yield of 1.63×10^5% and high photoresponsivity of 395 A W^{-1} were achieved at 300 nm in an In_2Se_3 phototransistor.[98]

Table 4. Performance parameters of 2D semiconductors beyond atomically thin MoS_2.

Sample	Photoresponsivity [mA W^{-1}]	Response time [ms]	Detecting λ [nm]	Reference
1L WS_2 a)	18.8	<4.5	532	[126]
6 nm WS_2 a)	0.092	5.3	457–647	[111]
42 nm WS_2 b)	5700–8.84×10^5	<20 ms	633	[124]
Multilayer WS_2 a)	700 at 635 nm	4100–9900	370–1064	[127]
1L $MoSe_2$ a)	13	60	532	[128]
20 nm $MoSe_2$ b)	9.71×10^4	15–30	532	[129]
20 nm $MoSe_2$ a)	9.37×10^4	400	638	[130]
1L WSe_2 b)	210 at 830 nm	–	512–850	[61]
1L WSe_2 a)	171 at 550 nm	<23	500–800	[131]
3L WSe_2 b)	100 at 532 nm	0.04	532	[132]
120 nm BP b)	20 at 532 nm; 5 at 1550 nm	–	532; 1550	[115]
Multilayer BP b)	4.8 at 640 nm	1	640; 885; 940	[114]
Multilayer GaTe b)	10^7	6	532	[116]
Multilayer GaSe b)	2800 at 254 nm	20	254–700	[125]
Multilayer GaS b)	1.92×10^4 at 254 nm	<30	254–610	[120]
10 nm In_2Se_3 b)	3.95×10^5 at 300 nm	18	300–1100	[98]
1L $ReSe_2$ b)	9.5×10^4	34–68	633	[133]
Multilayer SnS_2 a)	310–2000 at 450 nm	42	450	[122]
80 nm SnS_2 a)	8.8 at 457 nm	0.005	457; 633	[134]

a)CVD-grown samples; b)Exfoliated samples.

3.3. Photodetectors Based on vdW Heterostructures

vdW heterostructures can be formed by integrating 2D semiconductors with 0D, 1D, 2D, and 3D materials, which enriches the material platform for the development of diverse photodetection devices, as listed in **Table 5**. The 2D–0D vdW heterostructure consisting of 1L WS_2 and PbS quantum dots (QDs) was employed to make a photodetector working in the infrared range (i.e., 808 nm), where a high photoresponsivity of ≈14 A W^{-1} and fast response times (≈0.2 ms) were achieved (**Figure 8**a).[135] Moreover, a photodetector using heterostructures consisting of multilayer MoS_2 and PbS QDs was fabricated and operated in the broad spectral range from visible to infrared wavelengths (i.e., 400–1500 nm), demonstrating much higher photoresponsivity than those of photodetectors solely employing MoS_2 or PbS QDs.[136] Furthermore, by taking the advantages of the different absorption features of the two materials, an ultraviolet to near-infrared photoresponse was achieved in a flexible photodetector employing a hybrid of 2D MoS_2 nanosheets and carbon QDs, where the typical responsivities in the ultraviolet, visible, and near-infrared ranges were 8.4, 18.12, and 2.62 mA W^{-1}, respectively.[137] By vertically stacking n-type 1L MoS_2 and p-type single-walled carbon nanotubes (SWCNTs), a gate-tunable phototransistor based on such 2D–1D heterojunctions was demonstrated, exhibiting a fast photoresponse (<15 μs) together with an external quantum efficiency of 25%.[138] Moreover, a very broadband photoresponse from 400 to 950 nm was demonstrated in a phototransistor based on a 2D–1D vdW heterojunction, which was formed by covering a single n-type ZnO nanowire with p-type multilayer WSe_2 (Figure 8b).[139] Interestingly, after preparing the mixture of 2D MoS_2 nanoflakes and discrete 1D V_2O_5 nanowires on the

© 2018 WILEY-VCH Verlag GmbH & Co. KGaA, Weinheim

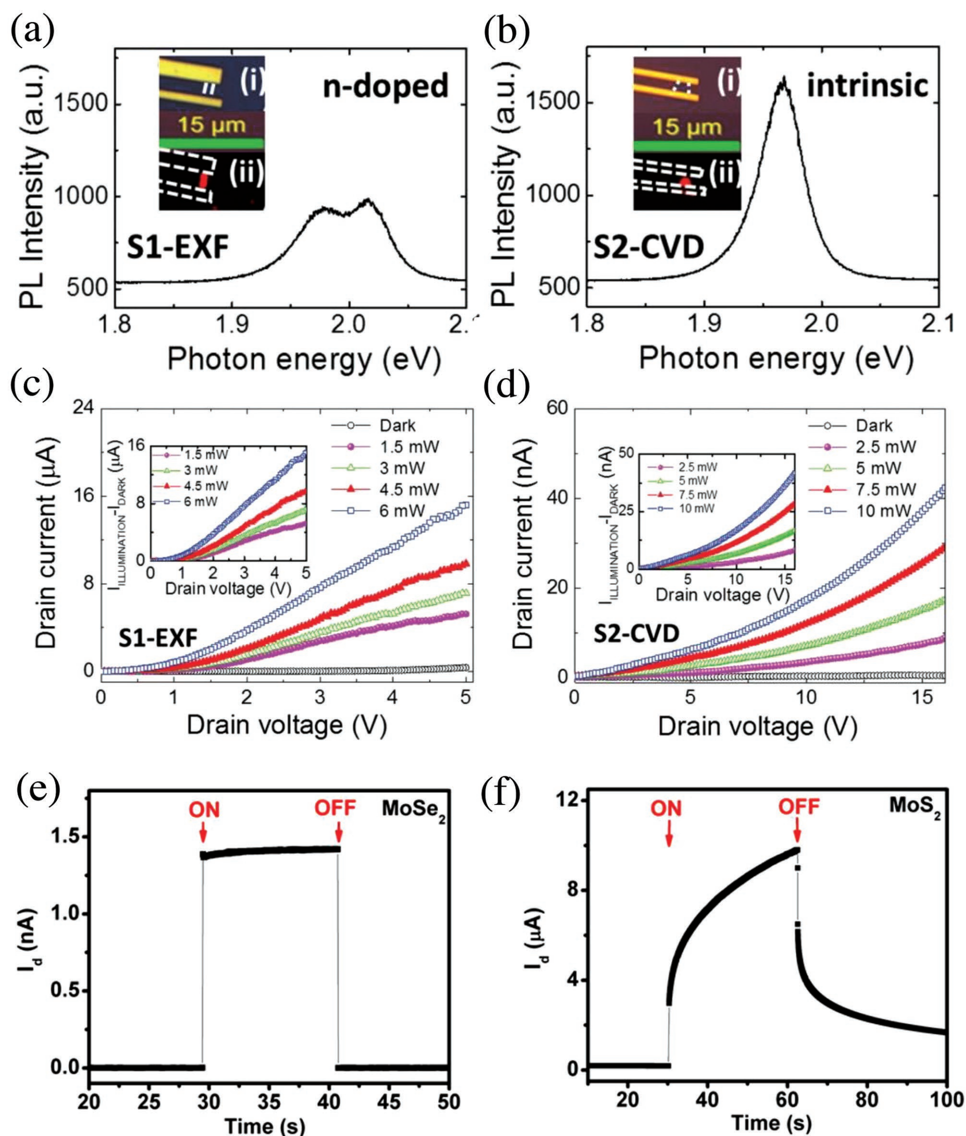

Figure 7. a) PL spectrum of a phototransistor based on exfoliated 1L WS_2 together with optical and fluorescence images (the inset). b) PL spectrum of a field-effect transistor based on CVD-grown 1L WS_2 together with optical and fluorescence images (the inset). c,d) Excitation power–dependent *I–V* curves of field-effect transistors based on exfoliated (c) and CVD-grown (d) 1L WS_2, where the insets illustrate the extracted drain currents caused by illumination. a–d) Reproduced with permission.[112] Copyright 2014, American Institute of Physics. e,f) Comparison of time-resolved photoresponse behaviors of the photodetectors based on CVD-grown 1L $MoSe_2$ (e) at excitation power of 0.59 W cm^{-2} (e) and 1L MoS_2 at excitation power of 0.31 W cm^{-2} (f). e,f) Reproduced with permission.[113] Copyright 2014, American Chemical Society.

aluminum foil, an enhanced broadband photoresponse has been realized on a flexible platform.[140] Considerable efforts have been made to fabricate photodetectors based on 2D–2D vdW heterojunctions. The photoresponse properties of atomically thin p-WSe_2/n-MoS_2 heterojunctions have been systematically investigated, which strongly depend on the thickness of each composite layer, the interlayer carrier tunneling, and the collection efficiency of photoexcited carriers.[53] A phototransistor using a heterostructure made of multilayer MoS_2 and 1L graphene was demonstrated to be possibly used for multifunctional memory devices, where an ultrahigh photoresponsivity was obtained at RT.[141] Particularly, the broadband photoresponse caused by interlayer excitons was studied in a phototransistor based on a p–n junction of 1L $MoSe_2$/1L WSe_2, enabled by dual back-gate electrodes (Figure 8c), where the photocurrent due to such interlayer excitons was two order smaller than that caused by intralayer excitons.[142] Furthermore, by preparing the vertical 2D–3D heterojunction with n-type 1L MoS_2 and p-type bulk Si (Figure 8d), a phototransistor based on this junction showed promising application prospects in solar-light harvesting, in view of its broad photoresponse from 500 to 1000 nm with the external quantum efficiency of 4.4%.[59] Photodetectors based on the multilayer WS_2/n-Si bulk heterojunction showed a significantly enhanced external quantum efficiency of >200%, owing to the abrupt heterojunction formation.[143] In addition, by

© 2018 WILEY-VCH Verlag GmbH & Co. KGaA, Weinheim

Table 5. Performance parameters of photodetectors based on vdW heterostructures.

Sample	Photoresponsivity [mA W^{-1}]	Response time [ms]	Detecting λ [nm]	Reference
$1LWS_2$[a)]/PbS QDs	1.4×10^4	0.15–0.23	808	[135]
2L MoS_2[a)]/PbS QDs	6×10^8	300–400	400–1500	[136]
1L MoS_2[b)]/SWCNTs	>100 at 650 nm	<15	500–1100	[138]
12 nm WSe_2[b)]/ZnO NW	670 at 520 nm	<50	400–950	[139]
1L MoS_2[b)]/rhodamine 6G	1170 at 520 nm	2300	405–980	[145]
1L MoS_2[b)]/G	10^{13}	1000	635	[141]
Graphene/1L MoS_2[b)]/graphene	220 at 488 nm	<0.05	458–633	[146]
1L MoS_2[b)]/1L WSe_2[b)]	2	–	532	[53]
Graphene/1L MoS_2[b)]/1L WSe_2[a)]/graphene	10 at 532 nm	–	500–800	[53]
Graphene/10 nm MoS_2[b)]/9 nm WSe_2[b)]/graphene	120 at 532 nm	–	500–825	[53]
1L MoS_2[a)]/hBN/graphene	0.3	1.1×10^4	500–700	[147]
1L MoS_2[a)]/11 nm BP[b)]	418	–	633	[148]
3.5 nm MoS_2[b)]/4.5 nm GaTe[b)]	1365	<10	633	[149]
1L MoS_2[b)]/Si	7200 at 365 nm	66–74	365–650	[150]
25 nm MoS_2[b)]/320 nm perovskite	2.12×10^7 at 520 nm	4000–7000	520–850	[151]

[a)]CVD-grown samples; [b)]Exfoliated samples.

mixing 3D nanostructured MoS_2 grown on cellulose paper with ZnS sub-microspheres, large-area flexible photodetectors based on such composites were demonstrated, presenting a broadband photoresponse in the range from the UV to the near-infrared.[144]

4. Challenges and Opportunities

The technological development of light sources and photodetectors based on 2D semiconductors has been reviewed. Although significant research progress has been made, there are still critical challenges, limiting the large-scale practicality and the industrial applications of 2D semiconductor–enabled light-emitting and photodetecting devices.

In the aspect of light sources, one remaining challenge is regarding the finite emission colors of present 2DLEDs, which limits their further practical applications for displays and illumination. Up to now, the main emission of the reported 2DLEDs[49,61–63,69] has covered the orange, red, and near-infrared spectral ranges, while 2DLEDs dominantly emitting from the ultraviolet to yellow wavelengths are still lacking. In particular, blue and green 2DLEDs are highly desired to realize 2D semiconductor–based full-color displays and while-light illumination. The second limiting factor is that the external quantum efficiencies of most 2DLEDs (≤10%)[49,61–63,68,69] are still very low with respect to those (e.g., 75%)[152,153] of conventional LEDs based on III–V semiconductors. Further investigation can lead to the improvement of internal quantum efficiencies of the emitting media and the optimization of device structures to increase the extraction efficiency. Note that the superacid treatments of some 2D semiconductors have shown dramatically enhanced quantum yields.[56,58]

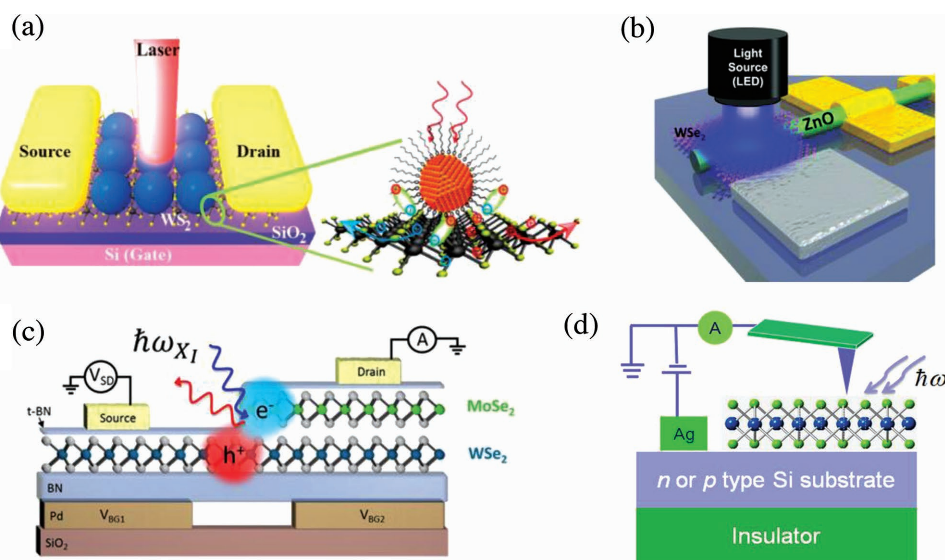

Figure 8. a) Schematic of photodetector based on a 2D–OD heterostructure made of 1L WS_2 and PbS QDs. The inset shows the zoom-in local structure. Reproduced with permission.[135] Copyright 2017, American Chemical Society. b) Schematic of photodetector based on a 2D–1D heterostructure based on multilayer WSe_2 and a ZnO nanowire. Reproduced with permission.[139] Copyright 2017, Wiley-VCH. c) Schematic of photodetector based on a 2D–2D heterostructure employing 1L WSe_2 and $MoSe_2$. Reproduced with permission.[142] Copyright 2017, American Chemical Society. d) Schematic of photodetector based on a 2D–3D heterostructure formed by 1L MoS_2 and n- or p-Si. Reproduced with permission.[150] Copyright 2014, Springer Nature.

© 2018 WILEY-VCH Verlag GmbH & Co. KGaA, Weinheim

Third, the fabrication of most reported 2DLEDs[24,49,59–63,68,69] typically relies on the individual transfer technique of mechanically exfoliated small flakes of 2D semiconductors, where the individual transfer and the exfoliated flakes are not compatible with the industrial purpose of large integration. Hence, controllable patterning and assembly of wafer-scale 2D semiconductors onto the targeted region need to be further developed, which are highly required for realistic lighting applications. Indeed, EL was observed from CVD-grown 1L WS_2, WSe_2, and MoS_2,[70,80] which moved a step toward making scalable 2DLEDs. Furthermore, the efficiency, purity, indistinguishability, and emission direction of single photons from 2DQLEDs can be further improved by additional structural designs, like the resonant microcavity.[154,155] Finally, previous investigations of 2D semiconductor lasers were demonstrated under optical pumping,[51,52,82,84–86] while electrically driven 2D semiconductor lasing is still highly demanded in order to fit well with the established Si-based photonic applications.

Diverse photodetectors with high photoresponsivity and broad response have been demonstrated by using 2D semiconductors and their vdW heterostructures. Nevertheless, the response times of most 2D semiconductor photodetectors[93,95,103,105,111,130] are significantly slower than those (<1 ns) of ultrafast Si,[156,157] Ge,[158,159] and InGaAs[160,161] photodiodes, which limit their promising applications for the high-speed (>1 GHz) photodetection required in typical fiber-optic communication. Additional designs and structural optimization may be helpful to improve the photoresponse speed. For instance, a fast response from ultrathin InSe was demonstrated in an avalanche photodetector employing a double Schottky barrier.[162] Furthermore, the development of on-chip optical receivers based on 2D semiconductors working in the spectral windows of optical interconnects is a very promising research frontier, which will contribute to a new device system for realizing optical computing.

More generally, research into light sources and photodetectors based on 2D semiconductors will boost new-generation optoelectronic applications and bring fascinating features into the present semiconductor lighting and photosensing technologies. The following research aspects deserve more attention: i) low-power and highly compact light sources and optical receivers for on-chip optical interconnects and quantum information; ii) full-color displays and while-light illumination based on 2DLEDs with enhanced brightness; iii) ultrathin, flexible, and/or transparent lighting, displays, and photodetectors for wearable and transparent electronics.

Acknowledgements

This work was mainly supported by the Singapore Ministry of Education (MOE) Tier 1 RG100/15 and Tier 1 RG199/17. C.C. acknowledges the support from the National Young 1000 Talent Plan of China, the Shanghai Municipal Natural Science Foundation (No. 16ZR1402500), the National Natural Science Foundation of China (No. 61774040), and the Opening Project of State Key Laboratory of Functional Materials for Informatics, Shanghai Institute of Microsystem and Information Technology, Chinese Academy of Sciences. W.H. acknowledges the support from the Natural Science Foundation of Jiangsu Province (BM2012010), the Priority Academic Program Development of Jiangsu Higher Education Institutions (YX03001), the Ministry of Education of China (IRT1148), the Synergetic Innovation Center for Organic Electronics and Information Displays (61136003), the National Natural Science Foundation of China (51173081), and the Fundamental Studies of Perovskite Solar Cells (2015CB932200).

Conflict of Interest

The authors declare no conflict of interest.

Keywords

2D semiconductors, lasers, light-emitting diodes, photodetectors

Received: January 30, 2018
Revised: February 24, 2018
Published online: May 2, 2018

[1] K. S. Novoselov, A. K. Geim, S. V. Morozov, D. Jiang, Y. Zhang, S. V. Dubonos, I. V. Grigorieva, A. A. Firsov, *Science* **2004**, *306*, 666.
[2] K. S. Novoselov, D. Jiang, F. Schedin, T. J. Booth, V. V. Khotkevich, S. V. Morozov, A. K. Geim, *Proc. Natl. Acad. Sci. USA* **2005**, *102*, 10451.
[3] C. Berger, Z. M. Song, T. B. Li, X. B. Li, A. Y. Ogbazghi, R. Feng, Z. T. Dai, A. N. Marchenkov, E. H. Conrad, P. N. First, W. A. de Heer, *J. Phys. Chem. B* **2004**, *108*, 19912.
[4] K. F. Mak, C. Lee, J. Hone, J. Shan, T. F. Heinz, *Phys. Rev. Lett.* **2010**, *105*, 136805.
[5] A. Splendiani, L. Sun, Y. B. Zhang, T. S. Li, J. Kim, C. Y. Chim, G. Galli, F. Wang, *Nano Lett.* **2010**, *10*, 1271.
[6] Q. H. Wang, K. Kalantar-Zadeh, A. Kis, J. N. Coleman, M. S. Strano, *Nat. Nanotechnol.* **2012**, *7*, 699.
[7] M. Chhowalla, H. S. Shin, G. Eda, L. J. Li, K. P. Loh, H. Zhang, *Nat. Chem.* **2013**, *5*, 263.
[8] X. D. Xu, W. Yao, D. Xiao, T. F. Heinz, *Nat. Phys.* **2014**, *10*, 343.
[9] G. Froehlicher, E. Lorchat, S. Berciaud, *Phys. Rev. B* **2016**, *94*, 085429.
[10] J. Z. Shang, X. N. Shen, C. X. Cong, N. Peimyoo, B. C. Cao, M. Eginligil, T. Yu, *ACS Nano* **2015**, *9*, 647.
[11] K. F. Mak, K. L. He, C. Lee, G. H. Lee, J. Hone, T. F. Heinz, J. Shan, *Nat. Mater.* **2013**, *12*, 207.
[12] P. Tonndorf, R. Schmidt, P. Bottger, X. Zhang, J. Borner, A. Liebig, M. Albrecht, C. Kloc, O. Gordan, D. R. T. Zahn, S. M. de Vasconcellos, R. Bratschitsch, *Opt. Express* **2013**, *21*, 4908.
[13] J. S. Ross, S. F. Wu, H. Y. Yu, N. J. Ghimire, A. M. Jones, G. Aivazian, J. Q. Yan, D. G. Mandrus, D. Xiao, W. Yao, X. D. Xu, *Nat. Commun.* **2013**, *9*, 268.
[14] W. J. Zhao, Z. Ghorannevis, L. Q. Chu, M. L. Toh, C. Kloc, P. H. Tan, G. Eda, *ACS Nano* **2013**, *7*, 791.
[15] X. M. Wang, A. M. Jones, K. L. Seyler, V. Tran, Y. C. Jia, H. Zhao, H. Wang, L. Yang, X. D. Xu, F. N. Xia, *Nat. Nanotechnol.* **2015**, *10*, 517.
[16] C. S. Jung, F. Shojaei, K. Park, J. Y. Oh, H. S. Im, D. M. Jang, J. Park, H. S. Kang, *ACS Nano* **2015**, *9*, 9585.
[17] K. S. Novoselov, A. Mishchenko, A. Carvalho, A. H. C. Neto, *Science* **2016**, *353*, 461.
[18] G. Cassabois, P. Valvin, B. Gil, *Nat. Photonics* **2016**, *10*, 262.
[19] F. N. Xia, H. Wang, D. Xiao, M. Dubey, A. Ramasubramaniam, *Nat. Photonics* **2014**, *8*, 899.

© 2018 WILEY-VCH Verlag GmbH & Co. KGaA, Weinheim

[20] A. Ramasubramaniam, *Phys. Rev. B* **2012**, *86*, 115409.
[21] W. C. Jin, P. C. Yeh, N. Zaki, D. T. Zhang, J. T. Sadowski, A. Al-Mahboob, A. M. van der Zande, D. A. Chenet, J. I. Dadap, I. P. Herman, P. Sutter, J. Hone, R. M. Osgood, *Phys. Rev. Lett.* **2013**, *111*, 106801.
[22] D. Xiao, G. B. Liu, W. X. Feng, X. D. Xu, W. Yao, *Phys. Rev. Lett.* **2012**, *108*, 196802.
[23] D. Y. Qiu, F. H. da Jornada, S. G. Louie, *Phys. Rev. Lett.* **2013**, *111*, 216805.
[24] R. S. Sundaram, M. Engel, A. Lombardo, R. Krupke, A. C. Ferrari, P. Avouris, M. Steiner, *Nano Lett.* **2013**, *13*, 1416.
[25] Z. Y. Yin, H. Li, H. Li, L. Jiang, Y. M. Shi, Y. H. Sun, G. Lu, Q. Zhang, X. D. Chen, H. Zhang, *ACS Nano* **2012**, *6*, 74.
[26] K. F. Mak, J. Shan, *Nat. Photonics* **2016**, *10*, 216.
[27] K. F. Mak, K. L. He, J. Shan, T. F. Heinz, *Nat. Nanotechnol.* **2012**, *7*, 494.
[28] O. L. Sanchez, D. Ovchinnikov, S. Misra, A. Allain, A. Kis, *Nano Lett.* **2016**, *16*, 5792.
[29] T. Cao, G. Wang, W. P. Han, H. Q. Ye, C. R. Zhu, J. R. Shi, Q. Niu, P. H. Tan, E. Wang, B. L. Liu, J. Feng, *Nat. Commun.* **2012**, *3*, 887.
[30] A. M. Jones, H. Y. Yu, N. J. Ghimire, S. F. Wu, G. Aivazian, J. S. Ross, B. Zhao, J. Q. Yan, D. G. Mandrus, D. Xiao, W. Yao, X. D. Xu, *Nat. Nanotechnol.* **2013**, *8*, 634.
[31] X. X. Zhang, T. Cao, Z. G. Lu, Y. C. Lin, F. Zhang, Y. Wang, Z. Q. Li, J. C. Hone, J. A. Robinson, D. Smirnov, S. G. Louie, T. F. Heinz, *Nat. Nanotechnol.* **2017**, *12*, 883.
[32] G. Aivazian, Z. R. Gong, A. M. Jones, R. L. Chu, J. Yan, D. G. Mandrus, C. W. Zhang, D. Cobden, W. Yao, X. Xu, *Nat. Phys.* **2015**, *11*, 148.
[33] A. Srivastava, M. Sidler, A. V. Allain, D. S. Lembke, A. Kis, A. Imamoglu, *Nat. Phys.* **2015**, *11*, 141.
[34] D. MacNeill, C. Heikes, K. F. Mak, Z. Anderson, A. Kormanyos, V. Zolyomi, J. Park, D. C. Ralph, *Phys. Rev. Lett.* **2015**, *114*, 037401.
[35] M. Koperski, K. Nogajewski, A. Arora, V. Cherkez, P. Mallet, J. Y. Veuillen, J. Marcus, P. Kossacki, M. Potemski, *Nat. Nanotechnol.* **2015**, *10*, 503.
[36] C. Chakraborty, L. Kinnischtzke, K. M. Goodfellow, R. Beams, A. N. Vamivakas, *Nat. Nanotechnol.* **2015**, *10*, 507.
[37] A. Srivastava, M. Sidler, A. V. Allain, D. S. Lembke, A. Kis, A. Imamoglu, *Nat. Nanotechnol.* **2015**, *10*, 491.
[38] Y. M. He, G. Clark, J. R. Schaibley, Y. He, M. C. Chen, Y. J. Wei, X. Ding, Q. Zhang, W. Yao, X. D. Xu, C. Y. Lu, J. W. Pan, *Nat. Nanotechnol.* **2015**, *10*, 497.
[39] E. J. Sie, J. McIver, Y. H. Lee, L. Fu, J. Kong, N. Gedik, *Nat. Mater.* **2015**, *14*, 290.
[40] X. Z. Liu, T. Galfsky, Z. Sun, F. N. Xia, E. C. Lin, Y. H. Lee, S. Kéna-Cohen, V. M. Menon, *Nat. Photonics* **2015**, *9*, 30.
[41] S. Dufferwiel, S. Schwarz, F. Withers, A. A. P. Trichet, F. Li, M. Sich, O. Del Pozo-Zamudio, C. Clark, A. Nalitov, D. D. Solnyshkov, G. Malpuech, K. S. Novoselov, J. M. Smith, M. S. Skolnick, D. N. Krizhanovskii, A. I. Tartakovskii, *Nat. Commun.* **2015**, *6*, 8579.
[42] S. Dufferwiel, T. P. Lyons, D. D. Solnyshkov, A. A. P. Trichet, F. Withers, S. Schwarz, G. Malpuech, J. M. Smith, K. S. Novoselov, M. S. Skolnick, D. N. Krizhanovskii, A. I. Tartakovskii, *Nat. Photonics* **2017**, *11*, 497.
[43] D. V. Tuan, B. Scharf, I. Zutic, H. Dery, *Phys. Rev. X* **2017**, *7*, 041040.
[44] Y. M. Shi, H. N. Li, L. J. Li, *Chem. Soc. Rev.* **2015**, *44*, 2744.
[45] C. R. Dean, A. F. Young, I. Meric, C. Lee, L. Wang, S. Sorgenfrei, K. Watanabe, T. Taniguchi, P. Kim, K. L. Shepard, J. Hone, *Nat. Nanotechnol.* **2010**, *5*, 722.
[46] A. Castellanos-Gomez, M. Buscema, R. Molenaar, V. Singh, L. Janssen, H. S. J. van der Zant, G. A. Steele, *2D Mater.* **2014**, *1*, 011002.
[47] Y. H. Lee, L. L. Yu, H. Wang, W. J. Fang, X. Ling, Y. M. Shi, C. T. Lin, J. K. Huang, M. T. Chang, C. S. Chang, M. Dresselhaus, T. Palacios, L. J. Li, J. Kong, *Nano Lett.* **2013**, *13*, 1852.
[48] J. S. Ross, P. Klement, A. M. Jones, N. J. Ghimire, J. Q. Yan, D. G. Mandrus, T. Taniguchi, K. Watanabe, K. Kitamura, W. Yao, D. H. Cobden, X. D. Xu, *Nat. Nanotechnol.* **2014**, *9*, 268.
[49] F. Withers, O. Del Pozo-Zamudio, A. Mishchenko, A. P. Rooney, A. Gholinia, K. Watanabe, T. Taniguchi, S. J. Haigh, A. K. Geim, A. I. Tartakovskii, K. S. Novoselov, *Nat. Mater.* **2015**, *14*, 301.
[50] Y. J. Zhang, T. Oka, R. Suzuki, J. T. Ye, Y. Iwasa, *Science* **2014**, *344*, 725.
[51] S. F. Wu, S. Buckley, J. R. Schaibley, L. F. Feng, J. Q. Yan, D. G. Mandrus, F. Hatami, W. Yao, J. Vuckovic, A. Majumdar, X. D. Xu, *Nature* **2015**, *520*, 69.
[52] Y. Ye, Z. J. Wong, X. F. Lu, X. J. Ni, H. Y. Zhu, X. H. Chen, Y. Wang, X. Zhang, *Nat. Photonics* **2015**, *9*, 733.
[53] C. H. Lee, G. H. Lee, A. M. van der Zande, W. C. Chen, Y. L. Li, M. Y. Han, X. Cui, G. Arefe, C. Nuckolls, T. F. Heinz, J. Guo, J. Hone, P. Kim, *Nat. Nanotechnol.* **2014**, *9*, 676.
[54] H. P. Komsa, A. V. Krasheninnikov, *Phys. Rev. B* **2012**, *86*, 241201(R).
[55] G. Wang, A. Chernikov, M. M. Glazov, T. F. Heinz, X. Marie, T. Amand, B. Urbaszek, *Rev. Mod. Phys.* **2018**, *90*, 021001.
[56] M. Amani, D. H. Lien, D. Kiriya, J. Xiao, A. Azcatl, J. Noh, S. R. Madhvapathy, R. Addou, K. C. Santosh, M. Dubey, K. Cho, R. M. Wallace, S. C. Lee, J. H. He, J. W. Ager, X. Zhang, E. Yablonovitch, A. Javey, *Science* **2015**, *350*, 1065.
[57] H. Kim, D. H. Lien, M. Amani, J. W. Ager, A. Javey, *ACS Nano* **2017**, *11*, 5179.
[58] M. Amani, P. Taheri, R. Addou, G. H. Ahn, D. Kiriya, D. H. Lien, J. W. Ager, R. M. Wallace, A. Jayey, *Nano Lett.* **2016**, *16*, 2786.
[59] O. Lopez-Sanchez, E. A. Llado, V. Koman, A. F. I. Morral, A. Radenovic, A. Kis, *ACS Nano* **2014**, *8*, 3042.
[60] Y. Ye, Z. L. Ye, M. Gharghi, H. Y. Zhu, M. Zhao, Y. Wang, X. B. Yin, X. Zhang, *Appl. Phys. Lett.* **2014**, *104*, 193508.
[61] B. W. H. Baugher, H. O. H. Churchill, Y. F. Yang, P. Jarillo-Herrero, *Nat. Nanotechnol.* **2014**, *9*, 262.
[62] A. Pospischil, M. M. Furchi, T. Mueller, *Nat. Nanotechnol.* **2014**, *9*, 257.
[63] F. Withers, O. Del Pozo-Zamudio, S. Schwarz, S. Dufferwiel, P. M. Walker, T. Godde, A. P. Rooney, A. Gholinia, C. R. Woods, P. Blake, S. J. Haigh, K. Watanabe, T. Taniguchi, I. L. Aleiner, A. K. Geim, V. I. Fal'ko, A. I. Tartakovskii, K. S. Novoselov, *Nano Lett.* **2015**, *15*, 8223.
[64] S. Jo, N. Ubrig, H. Berger, A. B. Kuzmenko, A. F. Morpurgo, *Nano Lett.* **2014**, *14*, 2019.
[65] L. Dobusch, S. Schuler, V. Perebeinos, T. Mueller, *Adv. Mater.* **2017**, *29*, 1701304.
[66] S. F. Wang, J. Y. Wang, W. J. Zhao, F. Giustiniano, L. Q. Chu, I. Verzhbitskiy, J. Z. Yong, G. Eda, *Nano Lett.* **2017**, *17*, 5156.
[67] R. Cheng, D. H. Li, H. L. Zhou, C. Wang, A. X. Yin, S. Jiang, Y. Liu, Y. Chen, Y. Huang, X. F. Duan, *Nano Lett.* **2014**, *14*, 5590.
[68] D. H. Li, R. Cheng, H. L. Zhou, C. Wang, A. X. Yin, Y. Chen, N. O. Weiss, Y. Huang, X. F. Duan, *Nat. Commun.* **2015**, *6*, 7509.
[69] C. H. Liu, G. Clark, T. Fryett, S. F. Wu, J. J. Zheng, F. Hatami, X. D. Xu, A. Majumdar, *Nano Lett.* **2017**, *17*, 200.
[70] J. Pu, T. Fujimoto, Y. Ohasi, S. Kimura, C. H. Chen, L. J. Li, T. Sakanoue, T. Takenobu, *Adv. Mater.* **2017**, *29*, 1606918.
[71] I. Aharonovich, D. Englund, M. Toth, *Nat. Photonics* **2016**, *10*, 631.
[72] E. Knill, *Nature* **2010**, *463*, 441.
[73] D. Bouwmeester, J. W. Pan, K. Mattle, M. Eibl, H. Weinfurter, A. Zeilinger, *Nature* **1997**, *390*, 575.
[74] E. Waks, K. Inoue, C. Santori, D. Fattal, J. Vuckovic, G. S. Solomon, Y. Yamamoto, *Nature* **2002**, *420*, 762.
[75] T. T. Tran, K. Bray, M. J. Ford, M. Toth, I. Aharonovich, *Nat. Nanotechnol.* **2016**, *11*, 37.

© 2018 WILEY-VCH Verlag GmbH & Co. KGaA, Weinheim

[76] C. Palacios-Berraquero, M. Barbone, D. M. Kara, X. L. Chen, I. Goykhman, D. Yoon, A. K. Ott, J. Beitner, K. Watanabe, T. Taniguchi, A. C. Ferrari, M. Atature, *Nat. Commun.* **2016**, *7*, 12978.
[77] S. Schwarz, A. Kozikov, F. Withers, J. K. Maguire, A. P. Foster, S. Dufferwiel, L. Hague, M. N. Makhonin, L. R. Wilson, A. K. Geim, K. S. Novoselov, A. I. Tartakovskii, *2D Mater.* **2016**, *3*, 025038.
[78] G. Clark, J. R. Schaibley, J. Ross, T. Taniguchi, K. Watanabe, J. R. Hendrickson, S. Mou, W. Yao, X. D. Xu, *Nano Lett.* **2016**, *16*, 3944.
[79] M. Onga, Y. J. Zhang, R. Suzuki, Y. Iwasa, *Appl. Phys. Lett.* **2016**, *108*, 073107.
[80] W. H. Yang, J. Z. Shang, J. P. Wang, X. N. Shen, B. C. Cao, N. Peimyoo, C. J. Zou, Y. Chen, Y. L. Wang, C. X. Cong, W. Huang, T. Yu, *Nano Lett.* **2016**, *16*, 1560.
[81] Y. Ye, J. Xiao, H. L. Wang, Z. L. Ye, H. Y. Zhu, M. Zhao, Y. Wang, J. H. Zhao, X. B. Yin, X. Zhang, *Nat. Nanotechnol.* **2016**, *11*, 597.
[82] O. Salehzadeh, M. Djavid, N. H. Tran, I. Shih, Z. Mi, *Nano Lett.* **2015**, *15*, 5302.
[83] N. Peimyoo, J. Z. Shang, C. X. Cong, X. N. Shen, X. Y. Wu, E. K. L. Yeow, T. Yu, *ACS Nano* **2013**, *7*, 10985.
[84] J. Z. Shang, C. X. Cong, Z. L. Wang, N. Peimyoo, L. S. Wu, C. J. Zou, Y. Chen, X. Y. Chin, J. P. Wang, C. Soci, W. Huang, T. Yu, *Nat. Commun.* **2017**, *8*, 543.
[85] Y. Z. Li, J. X. Zhang, D. D. Huang, H. Sun, F. Fan, J. B. Feng, Z. Wang, C. Z. Ning, *Nat. Nanotechnol.* **2017**, *12*, 987.
[86] H. Fang, J. Liu, H. Li, L. Zhou, L. Liu, J. Li, X. Wang, T. F. Krauss, Y. Wang, *arXiv:1710.01591v1* **2017**.
[87] L. Britnell, R. M. Ribeiro, A. Eckmann, R. Jalil, B. D. Belle, A. Mishchenko, Y. J. Kim, R. V. Gorbachev, T. Georgiou, S. V. Morozov, A. N. Grigorenko, A. K. Geim, C. Casiraghi, A. H. Castro Neto, K. S. Novoselov, *Science* **2013**, *340*, 1311.
[88] H. J. Tan, Y. Fan, Y. Q. Zhou, Q. Chen, W. S. Xu, J. H. Warner, *ACS Nano* **2016**, *10*, 7866.
[89] C. J. Shih, Q. H. Wang, Y. Son, Z. Jin, D. Blankschtein, M. S. Strano, *ACS Nano* **2014**, *8*, 5790.
[90] Z. H. Sun, H. X. Chang, *ACS Nano* **2014**, *8*, 4133.
[91] F. H. L. Koppens, T. Mueller, P. Avouris, A. C. Ferrari, M. S. Vitiello, M. Polini, *Nat. Nanotechnol.* **2014**, *9*, 780.
[92] M. M. Furchi, D. K. Polyushkin, A. Pospischil, T. Mueller, *Nano Lett.* **2014**, *14*, 6165.
[93] Q. S. Wang, J. W. Lai, D. Sun, *Opt. Mater. Express* **2016**, *6*, 2313.
[94] J. L. Wang, H. H. Fang, X. D. Wang, X. S. Chen, W. Lu, W. D. Hu, *Small* **2017**, *13*, 1700894.
[95] M. Buscema, J. O. Island, D. J. Groenendijk, S. I. Blanter, G. A. Steele, H. S. J. van der Zant, A. Castellanos-Gomez, *Chem. Soc. Rev.* **2015**, *44*, 3691.
[96] D. S. Tsai, K. K. Liu, D. H. Lien, M. L. Tsai, C. F. Kang, C. A. Lin, L. J. Li, J. H. He, *ACS Nano* **2013**, *7*, 3905.
[97] W. Choi, M. Y. Cho, A. Konar, J. H. Lee, G. B. Cha, S. C. Hong, S. Kim, J. Kim, D. Jena, J. Joo, S. Kim, *Adv. Mater.* **2012**, *24*, 5832.
[98] R. B. Jacobs-Gedrim, M. Shanmugam, N. Jain, C. A. Durcan, M. T. Murphy, T. M. Murray, R. J. Matyi, R. L. Moore, B. Yu, *ACS Nano* **2014**, *8*, 514.
[99] P. G. Hu, J. Zhang, M. N. Yoon, X. F. Qiao, X. Zhang, W. Feng, P. H. Tan, W. Zheng, J. J. Liu, X. N. Wang, J. C. Idrobo, D. B. Geohegan, K. Xiao, *Nano Res.* **2014**, *7*, 694.
[100] D. Jariwala, V. K. Sangwan, L. J. Lauhon, T. J. Marks, M. C. Hersam, *ACS Nano* **2014**, *8*, 1102.
[101] X. D. Duan, C. Wang, A. L. Pan, R. Q. Yu, X. F. Duan, *Chem. Soc. Rev.* **2015**, *44*, 8859.
[102] F. N. Xia, T. Mueller, Y. M. Lin, A. Valdes-Garcia, P. Avouris, *Nat. Nanotechnol.* **2009**, *4*, 839.
[103] O. Lopez-Sanchez, D. Lembke, M. Kayci, A. Radenovic, A. Kis, *Nat. Nanotechnol.* **2013**, *8*, 497.
[104] H. S. Lee, S. W. Min, Y. G. Chang, M. K. Park, T. Nam, H. Kim, J. H. Kim, S. Ryu, S. Im, *Nano Lett.* **2012**, *12*, 3695.
[105] X. D. Wang, P. Wang, J. L. Wang, W. D. Hu, X. H. Zhou, N. Guo, H. Huang, S. Sun, H. Shen, T. Lin, M. H. Tang, L. Liao, A. Q. Jiang, J. L. Sun, X. J. Meng, X. S. Chen, W. Lu, J. H. Chu, *Adv. Mater.* **2015**, *27*, 6575.
[106] W. J. Zhang, J. K. Huang, C. H. Chen, Y. H. Chang, Y. J. Cheng, L. J. Li, *Adv. Mater.* **2013**, *25*, 3456.
[107] N. Perea-Lopez, Z. Lin, N. R. Pradhan, A. Iniguez-Rabago, A. L. Elias, A. McCreary, J. Lou, P. M. Ajayan, H. Terrones, L. Balicas, M. Terrones, *2D Mater.* **2014**, *1*, 011004.
[108] M. Eginligil, B. C. Cao, Z. L. Wang, X. N. Shen, C. X. Cong, J. Z. Shang, C. Soci, T. Yu, *Nat. Commun.* **2015**, *6*, 7636.
[109] A. R. Klots, A. K. M. Newaz, B. Wang, D. Prasai, H. Krzyzanowska, J. H. Lin, D. Caudel, N. J. Ghimire, J. Yan, B. L. Ivanov, K. A. Velizhanin, A. Burger, D. G. Mandrus, N. H. Tolk, S. T. Pantelides, K. I. Bolotin, *Sci. Rep.* **2014**, *4*, 6608.
[110] Z. F. Yang, R. Grassi, M. Freitag, Y. H. Lee, T. Low, W. J. Zhu, *Appl. Phys. Lett.* **2016**, *108*, 083104.
[111] N. Perea-Lopez, A. L. Elias, A. Berkdemir, A. Castro-Beltran, H. R. Gutierrez, S. M. Feng, R. T. Lv, T. Hayashi, F. Lopez-Urias, S. Ghosh, B. Muchharla, S. Talapatra, H. Terrones, M. Terrones, *Adv. Funct. Mater.* **2013**, *23*, 5511.
[112] B. C. Cao, X. N. Shen, J. Z. Shang, C. X. Cong, W. H. Yang, M. Eginligil, T. Yu, *APL Mater.* **2014**, *2*, 116101.
[113] Y. H. Chang, W. Zhang, Y. Zhu, Y. Han, J. Pu, J. K. Chang, W. T. Hsu, J. K. Huang, C. L. Hsu, M. H. Chiu, T. Takenobu, H. Li, C. I. Wu, W. H. Chang, A. T. S. Wee, L. J. Li, *ACS Nano* **2014**, *8*, 8582.
[114] M. Buscema, D. J. Groenendijk, S. I. Blanter, G. A. Steele, H. S. J. van der Zant, A. Castellanos-Gomez, *Nano Lett.* **2014**, *14*, 3347.
[115] M. Engel, M. Steiner, P. Avouris, *Nano Lett.* **2014**, *14*, 6414.
[116] F. C. Liu, H. Shimotani, H. Shang, T. Kanagasekaran, V. Zolyomi, N. Drummond, V. I. Fal'ko, K. Tanigaki, *ACS Nano* **2014**, *8*, 752.
[117] X. F. Li, M. W. Lin, A. A. Puretzky, J. C. Idrobo, C. Ma, M. F. Chi, M. Yoon, C. M. Rouleau, I. I. Kravchenko, D. B. Geohegan, K. Xiao, *Sci. Rep.* **2014**, *4*, 5497.
[118] D. J. Xue, J. H. Tan, J. S. Hu, W. P. Hu, Y. G. Guo, L. J. Wan, *Adv. Mater.* **2012**, *24*, 4528.
[119] S. D. Lei, L. H. Ge, Z. Liu, S. Najmaei, G. Shi, G. You, J. Lou, R. Vajtai, P. M. Ajayan, *Nano Lett.* **2013**, *13*, 2777.
[120] P. A. Hu, L. F. Wang, M. Yoon, J. Zhang, W. Feng, X. N. Wang, Z. Z. Wen, J. C. Idrobo, Y. Miyamoto, D. B. Geohegan, K. Xiao, *Nano Lett.* **2013**, *13*, 1649.
[121] S. X. Yang, S. Tongay, Q. Yue, Y. T. Li, B. Li, F. Y. Lu, *Sci. Rep.* **2014**, *4*, 5442.
[122] J. Xia, D. D. Zhu, L. Wang, B. Huang, X. Huang, X. M. Meng, *Adv. Funct. Mater.* **2015**, *25*, 4255.
[123] W. S. Hwang, M. Remskar, R. S. Yan, V. Protasenko, K. Tahy, S. D. Chae, P. Zhao, A. Konar, H. L. Xing, A. Seabaugh, D. Jena, *Appl. Phys. Lett.* **2012**, *101*, 013107.
[124] N. J. Huo, S. X. Yang, Z. M. Wei, S. S. Li, J. B. Xia, J. B. Li, *Sci. Rep.* **2014**, *4*, 5209.
[125] P. A. Hu, Z. Z. Wen, L. F. Wang, P. H. Tan, K. Xiao, *ACS Nano* **2012**, *6*, 5988.
[126] C. Y. Lan, C. Li, Y. Yin, Y. Liu, *Nanoscale* **2015**, *7*, 5974.
[127] J. D. Yao, Z. Q. Zheng, J. M. Shao, G. W. Yang, *Nanoscale* **2015**, *7*, 14974.
[128] J. Xia, X. Huang, L. Z. Liu, M. Wang, L. Wang, B. Huang, D. D. Zhu, J. J. Li, C. Z. Gu, X. M. Meng, *Nanoscale* **2014**, *6*, 8949.
[129] A. Abderrahmane, P. J. Ko, T. V. Thu, S. Ishizawa, T. Takamura, A. Sandhu, *Nanotechnology* **2014**, *25*, 365202.
[130] C. Jung, S. M. Kim, H. Moon, G. Han, J. Kwon, Y. K. Hong, I. Omkaram, Y. Yoon, S. Kim, J. Park, *Sci. Rep.* **2015**, *5*, 15313.

© 2018 WILEY-VCH Verlag GmbH & Co. KGaA, Weinheim

[131] W. Zhang, M. H. Chiu, C. H. Chen, W. Chen, L. J. Li, A. T. S. Wee, *ACS Nano* **2014**, *8*, 8653.
[132] N. R. Pradhan, J. Ludwig, Z. G. Lu, D. Rhodes, M. M. Bishop, K. Thirunavukkuarasu, S. A. McGill, D. Smirnov, L. Balicas, *ACS Appl. Mater. Interfaces* **2015**, *7*, 12080.
[133] S. X. Yang, S. Tongay, Y. Li, Q. Yue, J. B. Xia, S. S. Li, J. B. Li, S. H. Wei, *Nanoscale* **2014**, *6*, 7226.
[134] G. X. Su, V. G. Hadjiev, P. E. Loya, J. Zhang, S. D. Lei, S. Maharjan, P. Dong, P. M. Ajayan, J. Lou, H. B. Peng, *Nano Lett.* **2015**, *15*, 506.
[135] Y. Yu, Y. T. Zhang, X. X. Song, H. T. Zhang, M. X. Cao, Y. L. Che, H. T. Dai, J. B. Yang, H. Zhang, J. Q. Yao, *ACS Photonics* **2017**, *4*, 950.
[136] D. Kufer, I. Nikitskiy, T. Lasanta, G. Navickaite, F. H. L. Koppens, G. Konstantatos, *Adv. Mater.* **2015**, *27*, 176.
[137] P. Sahatiya, S. S. Jones, S. Badhulika, *Appl. Mater. Today* **2018**, *10*, 106.
[138] D. Jariwala, V. K. Sangwan, C. C. Wu, P. L. Prabhumirashi, M. L. Geier, T. J. Marks, L. J. Lauhon, M. C. Hersam, *Proc. Natl. Acad. Sci. USA* **2013**, *110*, 18076.
[139] Y. T. Lee, P. J. Jeon, J. H. Han, J. Ahn, H. S. Lee, J. Y. Lim, W. K. Choi, J. D. Song, M.-C. Park, S. Im, D. K. Hwang, *Adv. Funct. Mater.* **2017**, *27*, 1703822.
[140] P. Sahatiya, C. S. Reddy K, S. Badhulika, *J. Mater. Chem. C* **2017**, *5*, 12728.
[141] K. Roy, M. Padmanabhan, S. Goswami, T. P. Sai, G. Ramalingam, S. Raghavan, A. Ghosh, *Nat. Nanotechnol.* **2013**, *8*, 826.
[142] J. S. Ross, P. Rivera, J. Schaibley, E. Lee-Wong, H. Y. Yu, T. Taniguchi, K. Watanabe, J. Q. Yan, D. Mandrus, D. Cobden, W. Yao, X. D. Xu, *Nano Lett.* **2017**, *17*, 638.
[143] R. K. Chowdhury, R. Maiti, A. Ghorai, A. Midya, S. K. Ray, *Nanoscale* **2016**, *8*, 13429.
[144] P. T. Gomathi, P. Sahatiya, S. Badhulika, *Adv. Funct. Mater.* **2017**, *27*, 1701611.
[145] S. H. Yu, Y. Lee, S. K. Jang, J. Kang, J. Jeon, C. Lee, J. Y. Lee, H. Kim, E. Hwang, S. Lee, J. H. Cho, *ACS Nano* **2014**, *8*, 8285.
[146] W. J. Yu, Y. Liu, H. L. Zhou, A. X. Yin, Z. Li, Y. Huang, X. F. Duan, *Nat. Nanotechnol.* **2013**, *8*, 952.
[147] H. Jeong, H. M. Oh, S. Bang, H. J. Jeong, S. J. An, G. H. Han, H. Kim, S. J. Yun, K. K. Kim, J. C. Park, Y. H. Lee, G. Lerondel, M. S. Jeong, *Nano Lett.* **2016**, *16*, 1858.
[148] Y. X. Deng, Z. Luo, N. J. Conrad, H. Liu, Y. J. Gong, S. Najmaei, P. M. Ajayan, J. Lou, X. F. Xu, P. D. Ye, *ACS Nano* **2014**, *8*, 8292.
[149] S. X. Yang, C. Wang, C. Ataca, Y. Li, H. Chen, H. Cai, A. Suslu, J. C. Grossman, C. B. Jiang, Q. Liu, S. Tongay, *ACS Appl. Mater. Interfaces* **2016**, *8*, 2533.
[150] Y. Li, C. Y. Xu, J. Y. Wang, L. Zhen, *Sci. Rep.* **2014**, *4*, 7186.
[151] D. H. Kang, S. R. Pae, J. Shim, G. Yoo, J. Jeon, J. W. Leem, J. S. Yu, S. Lee, B. Shin, J. H. Park, *Adv. Mater.* **2016**, *28*, 7799.
[152] S. Pimputkar, J. S. Speck, S. P. DenBaars, S. Nakamura, *Nat. Photonics* **2009**, *3*, 179.
[153] Y. Narukawa, M. Sano, T. Sakamoto, T. Yamada, T. Mukai, *Phys. Status Solidi A* **2008**, *205*, 1081.
[154] Y. M. He, Y. He, Y. J. Wei, D. Wu, M. Atature, C. Schneider, S. Hofling, M. Kamp, C. Y. Lu, J. W. Pan, *Nat. Nanotechnol.* **2013**, *8*, 213.
[155] X. Ding, Y. He, Z. C. Duan, N. Gregersen, M. C. Chen, S. Unsleber, S. Maier, C. Schneider, M. Kamp, S. Hofling, C. Y. Lu, J. W. Pan, *Phys. Rev. Lett.* **2016**, *116*, 020401.
[156] M. K. Emsley, O. Dosunmu, M. S. Unlu, *IEEE Photonics Technol. Lett.* **2002**, *14*, 519.
[157] H. C. Lee, B. Vanzeghbroeck, *IEEE Electron Device Lett.* **1995**, *16*, 175.
[158] S. Fama, L. Colace, G. Masini, G. Assanto, H. C. Luan, *Appl. Phys. Lett.* **2002**, *81*, 586.
[159] G. Dehlinger, S. J. Koester, J. D. Schaub, J. O. Chu, Q. C. Ouyang, A. Grill, *IEEE Photonics Technol. Lett.* **2004**, *16*, 2547.
[160] N. Shimizu, N. Watanabe, T. Furuta, T. Ishibashi, *IEEE Photonics Technol. Lett.* **1998**, *10*, 412.
[161] H. Ito, T. Furuta, S. Kodama, T. Ishibashi, *Electron. Lett.* **2000**, *36*, 1809.
[162] S. D. Lei, F. F. Wen, L. H. Ge, S. Najmaei, A. George, Y. J. Gong, W. L. Gao, Z. H. Jin, B. Li, J. Lou, J. Kono, R. Vajtai, P. Ajayan, N. J. Halas, *Nano Lett.* **2015**, *15*, 3048.

© 2018 WILEY-VCH Verlag GmbH & Co. KGaA, Weinheim